

# High Resolution Rydberg Spectroscopy of ultracold Rubidium Atoms

Axel Grabowski, Rolf Heidemann, Robert Low, Jürgen Stühler, and Tilman Pfau  
5. Physikalisches Institut, Universität Stuttgart, Pfaffenwaldring 57, 70550 Stuttgart, Germany  
(Dated: March 29, 2024)

We present experiments on two-photon excitation of  $^{87}\text{Rb}$  atoms to Rydberg states. For this purpose, two continuous-wave (cw)-laser systems for both 780 nm and 480 nm have been set up. These systems are optimized to a small linewidth (well below 1 MHz) to get both an efficient excitation process and good spectroscopic resolution. To test the performance of our laser system, we investigated the Stark splitting of Rydberg states. For  $n=40$  we were able to see the hyperfine levels splitting in the electrical field for different fine structure states. To show the ability of spatially selective excitation to Rydberg states, we excited rubidium atoms in an electrical field gradient and investigated both linewidths and lineshifts. Furthermore we were able to excite the atoms selectively from the two hyperfine ground states to Rydberg states. Finally, we investigated the Autler-Townes splitting of the  $5S_{1=2} \rightarrow 5P_{3=2}$  transition via a Rydberg state to determine the Rabi frequency of this excitation step.

## I. INTRODUCTION

During the last decades, a lot of studies have been performed on Rydberg atoms [1]. These experiments made use of atomic beams emitted from a thermal source. In the last years, methods of laser cooling [2] of atoms opened new ways to perform experiments on Rydberg states using atom samples at temperatures in the 100 K range. Such a system of ultracold Rydberg atoms is known as "frozen Rydberg gas" [3, 4]. The name is correlated to the fact, that there is nearly no thermal motion of the atoms during the time constant of the experiment. Typically, in the time for one experiment of  $\sim 10$  s, an atom moves about 1  $\mu\text{m}$  which is smaller than the mean interatomic distance. An interesting property of Rydberg atoms are the long-range dipole-dipole and van der Waals interactions. First investigations of the interaction among the atoms in such "frozen Rydberg" systems have started recently [5, 6, 7, 8, 9]. In these experiments, the interaction led to an increasing suppression of excitation as a function of increasing Rydberg atom density. This suppression mechanism is called van der Waals blockade, because the van der Waals interaction among the atoms prohibits further excitation by shifting the energy levels of neighboring atoms out of resonance with respect to the excitation lasers.

Rydberg atoms or mesoscopic ensembles of them are discussed in the context of quantum information processing [10, 11] as conditional logic gates based on the strong interaction between the atoms. To use Rydberg atoms in quantum computing, there are several tasks which have to be achieved first. In the proposal given by Jaksch et al. [10], there must be a possibility to arrange the atoms spatially in a defined way. This can either be done in optical [12] or magnetic lattices [13], where ground state atoms are captured. The quantum information is hereby stored in the hyperfine ground state of the atoms.

In this paper, we present experiments on the excitation of cold  $^{87}\text{Rb}$  atoms to Rydberg states. The atoms are first prepared in a magneto-optical trap (MOT) [2] and then excited in a two-photon two-color excitation step to a Rydberg state. For this purpose, a narrow linewidth cw-laser system for both wavelengths has been set up. Using this system, we investigated Rydberg excitation in the proximity of the  $n=40$  state. With the high spectroscopic resolution of our laser system, we were able to investigate the Stark splitting of the Rydberg states and could even resolve the state dependent hyperfine Stark splitting for different  $J$ -states.

For quantum computing purposes with Rydberg atoms [10] one has to be able to address the atoms individually in space (for example in an optical lattice). Due to the fact that the quantum information is stored in the hyperfine ground states, it is necessary to be able to excite the atoms from a defined ground state (in  $^{87}\text{Rb}$ ,  $F=1$  and  $F=2$ ) to the Rydberg state. For every quantum computing scheme, it is essential to conserve coherence during the operations. In case of using Rydberg atoms, this means that a coherent excitation of the atoms to Rydberg states is needed. To get to know the time constants of the experimental cycle, we measured the Rabi frequency of the lower transition of the two-photon excitation process. For this purpose, we investigated the Autler-Townes splitting of the  $5S_{1=2} \rightarrow 5P_{3=2}$  transition. This is done by probing the splitting of this splitted state with a narrow band excitation to a Rydberg state [14].

This paper is organized as follows: In section 2, we describe the experimental setup, especially the laser system for the Rydberg excitation and the detection of the atoms. In section 3, we give an example for the spectroscopic resolution and the overall stability of the system by measuring a Stark map in the vicinity of the  $n=40$  manifold. Section 4 presents experiments on the state- and spatially selective excitation. Beyond this, we report in section 5 on the measurements of the Rabi frequency on the  $5S_{1=2} \rightarrow 5P_{3=2}$  transition by observing the Autler-Townes splitting of this transition.

## II. EXPERIMENTAL SETUP AND COLD ATOM PREPARATION

### A. Vacuum system and magneto optical trap (MOT)

The experiments presented here are performed inside a vacuum chamber as shown in Fig. 1. The chamber consists of a steel tube with an inner diameter of 10 cm. In the radial direction, optical access is provided on three axes (4x CF-36 angles with windows and 2x CF-16 angles with windows). The bottom of the chamber is sealed with a large glass window of 175 mm in diameter. The MOT is built up as a reflection MOT [15] where two of the MOT beams are reflected from a reflective surface inside the vacuum chamber. The other MOT beams use one of the accessible axes of the chamber. One other axis of the chamber is used for fluorescence imaging of the atomic cloud. The magnetic quadrupole field for the MOT is produced by the current through a wire behind the gold covered copper plate inside the vacuum chamber superimposed with a homogeneous magnetic field produced by Helmholtz coils outside the chamber (U-type quadrupole) [16].

The rubidium for the MOT is provided by a dispenser (SEAS Getters) situated close to the atomic cloud and well shielded by a mesh cage to prohibit any disturbances in the electrical field inside the vacuum chamber. The pressure inside the vacuum chamber which is pumped by both a titanium sublimation pump and an ion pump is in the range of  $10^{-10}$  mbar.

Due to the fact, that Rydberg atoms are very sensitive to electrical fields [1], all sources for electrical stray fields

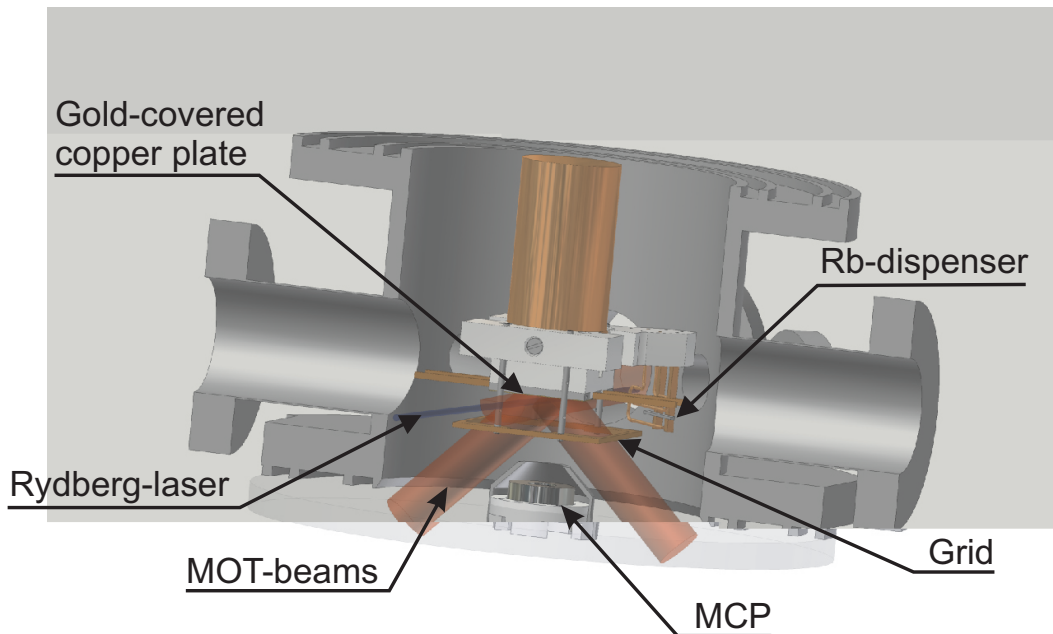


FIG. 1: Setup of the vacuum system with field plates and micro channel plate (MCP). Furthermore the laser beams for both MOT (red) and Rydberg excitation are drawn (blue beam in front). The gold covered copper plate and the copper grid are 10 mm apart from each other (middle of the picture) surrounding the MOT. The dispenser in the background is shielded by a cage. The MCP is situated in the middle of the vacuum chamber on the lower window.

inside the vacuum chamber have to be shielded as good as possible. To control the electrical field, we placed field plates inside the vacuum chamber around the MOT region. Here, we used the gold covered Cu plate which is likewise used for the reflection MOT as one field plate. A copper mesh (SPIFine Grid Mesh, 02199C-AG), sitting 1 cm below the copper plate forms the second field plate. The mesh has a high optical transmission of 85% and the size of the holes in the grid is only 234  $\mu$ m. These field plates enable us to apply a homogeneous electrical field and shield the MOT region from electric field gradients. By applying a voltage to these plates, we can generate an electrical field and are able to investigate the Stark interaction of the Rydberg atoms with it.

For the magneto optical trap, we use grating stabilized diode lasers in the Littrow configuration [17]. The MOT-laser is quasi-resonant to the  $5S_{1=2}$  ( $F=2$ ) !  $5P_{3=2}$  ( $F=3$ ) transition ( $\lambda = 780.248$  nm, see Fig. 2). It is stabilized via polarization spectroscopy on a crossover transition in the Rubidium spectrum [18], 133 MHz below the MOT transition. The laser light is afterwards amplified in a "slave" diode and then frequency shifted by an acousto-optical modulator (AOM). The frequency is usually detuned by  $-2$  with respect to the  $5S_{1=2}$  ( $F=2$ ) !  $5P_{3=2}$  ( $F=3$ )

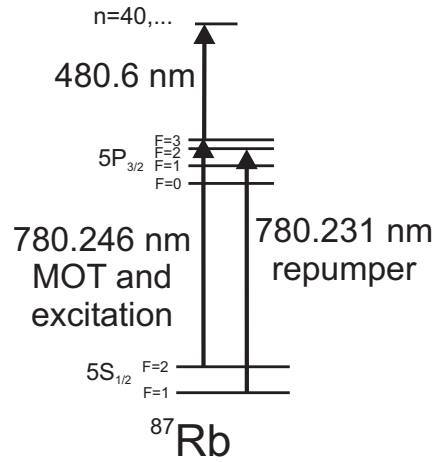


FIG. 2: Level scheme of  $^{87}\text{Rb}$  for cooling, trapping and Rydberg excitation.

transition. We end up with a total power of about 30 mW in the 3 MOT beams (all of them are retro-reflected). A second laser for the MOT, another grating stabilized diode laser is also locked on a crossover signal. This laser is shifted with an AOM in single pass to resonance with the  $5S_{1=2}$  ( $F=1$ )!  $5P_{3=2}$  ( $F=2$ ) transition ( $\lambda = 780.231$  nm, see Fig. 2). This second so-called repumper laser is needed because MOT atoms can be pumped to the lower hyperfine ground state by off-resonant excitation and are yet lost out of the MOT cycle. The repumper pumps these otherwise lost atoms back. It is superimposed with all the beams of the MOT laser. The AOMs in both of the beams can also be used for fast switching.

For the detection of the MOT atoms, a CCD camera outside the vacuum chamber is used to record both fluorescence and absorption images. The cloud is imaged with a 1:1 telescope to the camera. For the experiments presented here, only fluorescence pictures are taken. The number of atoms in the MOT can be calculated from these fluorescence pictures. The temperature of the atoms in the MOT can be determined by the time-of-flight expansion of the cloud. We usually operate the Rubidium dispenser at low currents of 4-4.5 A to prevent contamination of the vacuum chamber during the experiments. This leads to MOT atom numbers of  $10^6$  atoms at a density of  $10^{10}$  atoms/cm<sup>3</sup>. The temperature of the MOT is about 100-400 K.

### B. Rydberg laser system and Rydberg excitation

As shown in Fig. 2, two lasers with wavelengths of 780 nm and 480 nm are needed for the two-photon Rydberg excitation. For this purpose, we built up a laser system consisting of three diode lasers. For the 480 nm laser system the problem arises, that one wants to be able to stabilize the laser to every possible optical Rydberg transition between  $n=30$  and the ionization threshold. For this reason, we decided to stabilize a master laser to a reference resonator. This 30 cm long reference cavity is stabilized in length by means of a highly stable laser system. With this setup we gain the possibility to lock the laser on every resonator fringe, at a separation of 125 MHz. The fringe to lock on is first found with a wavemeter (Advantest TQ 8325, 100 MHz resolution) and afterwards by scanning the laser around the Rydberg resonance with an AOM. The laser system is built up as master-slave diode laser system at a wavelength around 960 nm. The master laser is as described before a cavity stabilized diode laser, which is locked to the reference cavity. The laser beam is afterwards frequency shifted with a 400 MHz AOM in double pass configuration, which allows us to vary the frequency of more than 250 MHz. After passing the AOM the beam seeds a 300 mW slave diode. If the master laser is locked onto the reference cavity it is possible to change the slave frequency by shifting the frequency of this AOM. With this setup, it is possible to generate every frequency in between two resonator fringes. Afterwards this 960 nm laser is frequency doubled in a home built doubling resonator by second harmonic generation in a KNbO<sub>3</sub> crystal, which yields a laser power of up to 20 mW at 480 nm after the cavity. This blue beam passes afterwards a 200 MHz AOM in single pass, which is used to regulate the power and to switch the beam.

With our laser system it is possible to scan the master-slave system unlocked to the cavity mode hop free about 6 GHz continuously (respectively frequency doubled 12 GHz). This scan range is limited by the available voltage range we apply to the piezo actuator in the master laser. By locking the laser to the reference cavity, the laser frequency is basically fixed but the frequency of the slave laser can be adjusted using the AOM between master and slave laser.

This way, we can scan the blue laser frequency about 500 MHz with high stability and small linewidth. For the 780 nm wavelength, an external cavity stabilized diode laser is used, locked to a rubidium cell via polarization spectroscopy. This laser has two applications. It is both used as a reference for stabilizing the length of our reference cavity and as first laser of the two-photon transition. This laser beam passes a 200 MHz double pass AOM which enables us to switch the laser fast, attenuate the beam and vary the laser frequency by more than 100 MHz. Depending on the line in the polarization spectroscopy spectrum we lock the laser to, we are able to work on the  $5S_{1=2} (F=2) \rightarrow 5P_{3=2} (F=3)$  resonance or up to 500 MHz blue detuned with respect to this transition. Both of the laser beams are guided to the experiment by two single mode optical fibers. After the optical fiber, we have typically 2.5 mW for the blue 480 nm beam and for the red 780 nm a power of about 7 mW. The red laser is collimated ( $1=e^2$  diameter of 0.95 mm) and shown onto the atomic cloud. The beam diameter is therefore larger than the MOT diameter. The blue laser is focused into the MOT cloud, and has a  $1=e^2$  diameter of 20  $\mu$ m. Its Rayleigh range of 3 mm is much larger than the size of the cloud. The overlapped pair of beams is irradiated inside the chamber. The beams are slightly tilted with an angle of about  $10^\circ$  with respect to the main axes of the chamber. Due to the selection rules for the two-photon excitation of atoms from the  $5S_{1=2}$  via the  $5P_{3=2}$  state to a Rydberg state only excitations to nS and nD states are dipole allowed transitions. However, even for small electrical fields the selection rules are no longer strict. Excitations to usually dipole transition forbidden states become possible because the target Rydberg states are no longer pure states but a mixture of different unperturbed states. Therefore, it is possible to excite atoms to P or even  $l > 3$  states in a non-vanishing electrical field. The  $l > 3$  states are called hydrogen-like states because the quantum defect for these states is negligible and they can be seen as pure hydrogen states showing a linear Stark effect with a permanent dipole moment. In contrast, the states with  $l < 3$  sustain for small electrical fields a quadratic Stark effect.

### C. Detection of the Rydberg atoms

For the detection of the Rydberg atoms, we use the way of field-ionizing the Rydberg atoms by an electrical field pulse and subsequent detection of the emerging ions with a micro channel plate (MCP). For the field ionization, the electrical field is switched on by a high speed, high voltage MOSFET switch (Type: Behlke HTS-6103 GSM). The typical rise time of this switch is 60 ns. We slow down the switching by a 2<sup>nd</sup> order low pass filter. This yields a rise time of the electrical field of 55 ns, which allows us to probe both ions and field-ionized Rydberg atoms selectively at different times. The ions are accelerated towards the MCP by the electrical field and are detected. The MCP signal is amplified in a home built I-U-converter circuit. The readout of the data is done by a computer with a digitizer card. The maximum sampling rate of the analog electronics and the digitizer card is 100 ns. For the calibration of the MCP, we directly photo-ionize the atoms from the MOT in an electrical field above the ionization threshold. This leads to a loss of atoms in the MOT due to ionization. After 100 ms the MOT atom number is decreased to a new steady state population which is related to the loading rate of the MOT and the loss rates. Measuring the reduced steady-state MOT atom number with the CCD-camera and recording simultaneously the number of produced ions with the MCP, we can calibrate the MCP efficiency. With this calibration, we are now able to calculate atom numbers from the MCP signal.

### D. Excitation sequence

During the Rydberg excitation all, the MOT and repump beams are switched off with the AOMs. After 100  $\mu$ s expansion time, the two collinear beams for Rydberg excitation are switched on simultaneously for a variable time between 100 ns and 1 ms. With a variable delay after the excitation pulse a voltage of 300 V is applied to the gold covered copper plate for field ionization of the Rydberg atoms. At the same time the copper grid is at ground potential, which yields an electrical field of 300 V/cm.

In Fig. 3 an example for the excitation sequence is shown. Here the excitation pulse is 100  $\mu$ s long. Already during the excitation pulse without an electrical field a signal on the MCP is seen (a). This signal is attributed to Rydberg-Rydberg collisions which lead to an ionization process among the Rydberg atoms [19]. Immediately after the excitation pulse is switched off, the electrical field is ramped up. At the beginning of this ramp a first bunch of ions is detected by the MCP (b). We assign this to ions that first remained in the atom cloud and are now pulled out by the rising electrical field of the ionization pulse. About 40  $\mu$ s later, a broad peak appears on the MCP signal (c), which is due to the field-ionized Rydberg atoms. The time until they reach the MCP is determined by the rising time of the electrical field. Only when the electrical field is high enough, the atoms are ionized and the ions are then accelerated towards the MCP. This peak is broadened due to l-changing collisions [20]. In the data shown in the next sections (see e.g.

g. 4), every data point consists of such a measurement as in g. 3. All the data of the single measurements are collected and stored. Afterwards the ion signal is integrated to get together with the calibration factor an absolute Rydberg atom number. The typical repetition rate of the experiment is 30 ms.

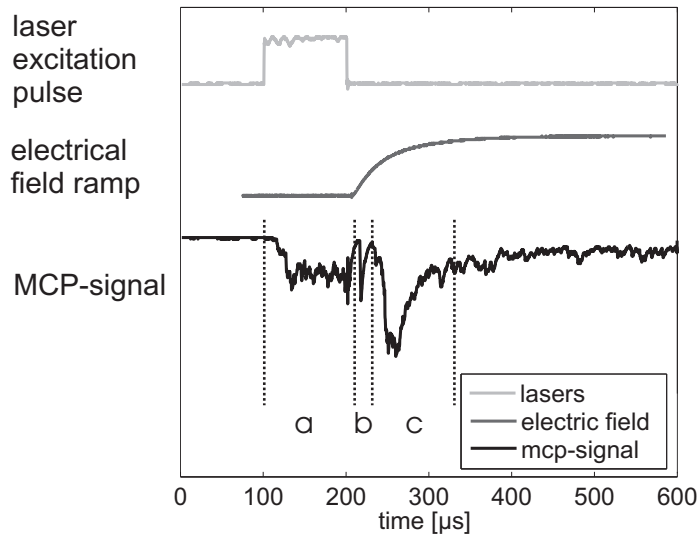


FIG. 3: Excitation sequence of the Rydberg atoms, field ionization pulse and corresponding MCP signal (see text).

### III. SPECTROSCOPY OF RYDBERG STATES, F SPLITTING OF THE RYDBERG STATES

Figure 4 shows a high resolution spectrum of the 41D doublet. For this experiment, we held the frequency of the red laser constant on resonance of the of the  $5S_{1=2}$  ( $F=2$ )  $\rightarrow$   $5P_{3=2}$  ( $F=3$ ) transition and changed both the frequency of the blue laser and the electrical field during excitation. In g. 4 a) the spectrum is taken with the unstabilized blue laser while in b) a spectrum obtained by scanning the locked laser system is shown. The electrical field applied across the interaction region during the excitation sequence is changed between 0 V/cm and 20 V/cm (a), respectively 10 V/cm (b). The color of the pictures indicates the signal strength (blue-low to red-high signal).

On the right hand side in g. 4 a) both the 41D doublet and the manifold of the  $n=40$  states can be found. As expected the intensity of the  $n=40$  lines is much weaker than the one of the D-lines, because these are  $l > 3$  states. Because some shift in the Rydberg lines cannot be excluded, we improved the stability by locking the laser onto the reference cavity. In g. 4 b) the measurement is done by changing the frequency of the AOM between master and slave laser. Thus we were able to scan the laser frequency with a stability of better than 1 MHz. So the splitting of the F-substates in the electrical field can be observed. The  $41D_{5=2}$ -level has the hyperfine substates  $F=1,2,3,4$ , the  $41D_{3=2}$  the F-states  $F=0,1,2,3$  ( $^{87}\text{Rb}$  has a nuclear spin of  $I=3/2$ ). We start the excitation from the  $5S_{1=2}$ ,  $F=2$  state via the  $5P_{3=2}$ ,  $F=3$  state. Therefore we can excite the atom in two different  $41D_{3=2}$ , respectively three different  $41D_{5=2}$ -states as can be seen in the picture. The additional shift of the  $5S_{1=2}$  and  $5P_{3=2}$  states is in the Stark maps negligible, because the polarizability of  $^{87}\text{Rb}$  in these low lying states is very small.

Beyond this, we measured the  $n=40$  manifold in the environment of the zero field crossing. From these data we could estimate the residual electrical field components to be less than 1 V/cm. The accuracy of the measurement was only limited by the small zero field excitation rate.

For small detunings and on resonance of the red transition, the linewidths of the entire transition we observe are basically determined by the linewidth of the lower transition. For large detunings from the  $5P_{3=2}$  state, the linewidth becomes smaller, because the intermediate state is adiabatically eliminated. The smallest linewidth we have measured so far was 2.2 MHz, although the laser linewidth is well below 1 MHz, determined from the laser stabilization signal. We attribute the residual line broadening to remaining magnetic fields of the MOT. The MOT has a magnetic field gradient of about 16 G/cm. The shift of the atoms in the  $S_{1=2}$  states is 0.7 MHz/G between two neighboring  $m_F$  substates ( $m_F = -2, \dots, 2$ ). At a MOT diameter of 500  $\mu\text{m}$  this yields a linewidth due to magnetic field broadening of 2.24 MHz which is in excellent agreement with our measurements.

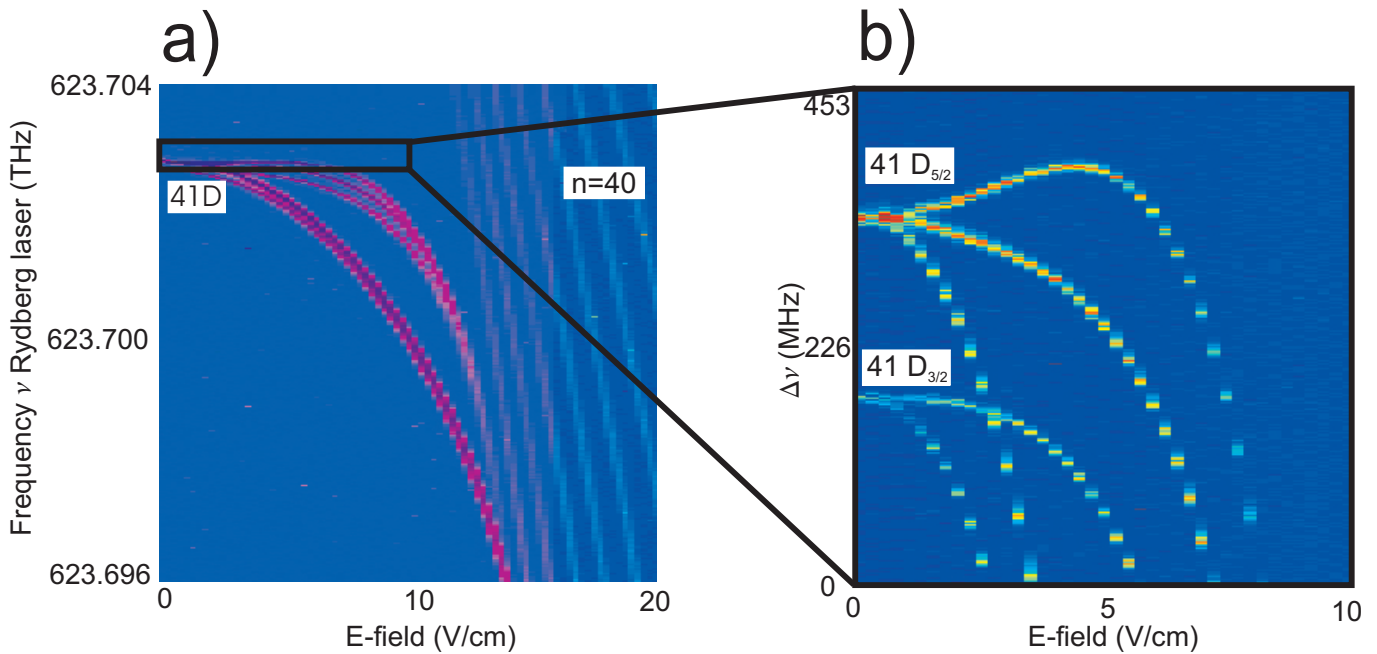


FIG. 4: Example for the spectroscopic resolution of the laser system. On the left hand side a Stark map scan is shown where the electrical field and the blue laser frequency is changed. On the right side is a scan of a smaller region with a higher resolution, revealing the F-Splitting of the Rydberg states in the electrical field.

#### IV. SPATIAL AND STATE SELECTIVE ADDRESSING OF RYDBERG STATES

##### A. Spatial selective Rydberg excitation

For quantum computing approaches with Rydberg atoms according to the proposal of D. Jaksch et al. [10] it is necessary to address the atoms individually at different positions in space. One possibility to do this is addressing via the Stark shift in electrical field gradients which links the resonance frequency of the atoms to their position. Here we present a demonstration experiment with Rydberg atoms in an electrical field gradient. For this purpose, we applied an electrical field gradient across our MOT and varied the position of the excitation lasers along this gradient. In Fig. 5 the  $41D_{3/2}$  and  $41D_{5/2}$  resonance lines are shown. The shift of the excitation beams by the diameter of the MOT cloud yields a line shift of 98 MHz and 75 MHz which is already larger than the linewidth of the broadened transitions. This broadening is due to electrical field gradient across the MOT. This is because the gradient we applied is not homogeneous in one direction, but also varies in the orthogonal direction. So each individual atom along the Rydberg excitation beam in the MOT is exposed to a different electrical field which leads to an inhomogeneous broadening. The measured linewidth of the two lines is 81 MHz, respectively 57 MHz which is much larger than the linewidth of the  $5S_{1/2}$  ( $F=2$ )!  $5P_{3/2}$  ( $F=3$ ) transition.

The origin for the different linewidths and shifts of the two transitions is the different slope of the two transitions in the electrical field as can be seen in Fig. 4. From the slope of this state in an electrical field and from the size of the cloud, the gradient of the electrical field in the direction of the movement of the laser can be estimated to be  $18.8 \text{ V/cm}^2$ . In future experiments, we will be able to apply a homogeneous electric field gradient which will shift the lines without the line broadening.

##### B. Hyperfine selective Rydberg excitation

In the quantum computing scheme with rubidium Rydberg atoms, the quantum information is stored in both of the hyperfine ground states ( $5S_{1/2}$   $F=1$ ,  $F=2$ ). For this reason, state selectivity of the ground states in the excitation scheme should be assured. This means that one of the  $5S_{1/2}$  ground states has to be accessible for the excitation to the Rydberg state, in a way that during the excitation, the other state is not affected. To test this, we excited from both hyperfine ground states to Rydberg states. In the experiment, we scanned the frequency of the blue laser across the resonance  $5P_{3/2}$ !  $41D$  and excited the atoms on the  $5S_{1/2}$ !  $5P_{3/2}$  transition with the MOT and the repumper

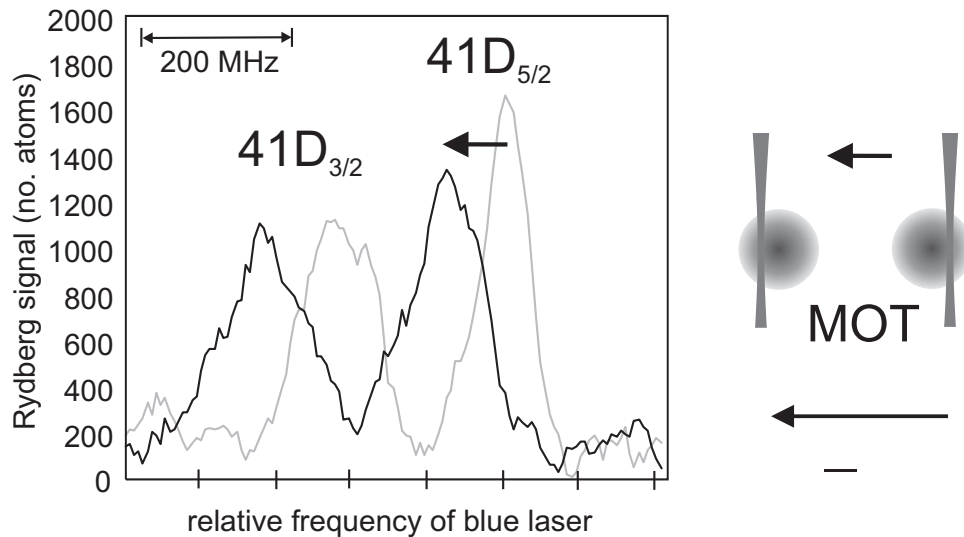


FIG. 5: Spatial dependent addressing of atoms of the cold cloud by using an electrical field gradient. The spatial addressing was done by moving the laser across the MOT. The frequency of the Rydberg lines is shifted according to the electrical field gradient.

laser as red laser system. The repumper light was resonant with the  $5S_{1=2} (F=1) \rightarrow 5P_{3=2} (F=1)$  transition. We did the excitation with and without optical pumping of the atoms to the  $F=1$  state before the Rydberg excitation. In an experiment where no atoms are actively pumped to the  $F=1$  state, an excitation is only possible from  $F=2$  state to the Rydberg state (e.g.,  $6, (3)$ ). No atoms can be excited from the  $F=1$  state to a Rydberg state (e.g.,  $6, (1)$ ). An excitation from the  $F=1$  state is only possible by actively pumping the atoms prior to the excitation process in the  $F=1$  state. This was done by switching on the repumper laser 300 ns earlier than the MOT laser before the Rydberg excitation. As shown in fig. 6 (2) and (4) the number of atoms excited from  $F=2$  to the  $n=41D$  shrinks (4) and an excitation from  $F=1$  to the  $n=40D$  states becomes possible (2). Since we could not completely switch on the AOM, we were not able to pump all the atoms in the  $F=1$  and it was not possible to fully deplete the  $F=2$  state. The measured frequency shift between the lines is about 460 MHz which is in a reasonable agreement with the theoretical prediction (423 MHz). The spectroscopic lines in this experiment are rather broad because of an electrical field gradient across the atom cloud. To improve the transfer efficiency, we will use in future experiments a Raman laser system to transfer the atoms between the hyperfine ground states.

## V. AUTLER-TOWNES SPLITTING

In an atomic ensemble that strongly interacts with a coherent light field, a new set of basis states for the coupled system can be found [21]. One consequence of this coupling is the well known Autler-Townes splitting [22]. The magnitude of the splitting is given by the Rabi frequency of the transition. In a three level system, it is possible to probe the Autler-Townes splitting of one state with a transition to an other state and therefore measure directly the Rabi frequency of the two-state system [14]. The knowledge of the Rabi frequency of our Rydberg system (for the red and for the blue transition) is necessary because for coherent excitation to Rydberg states, the Rabi frequency has to be larger than the inverse timescale of decoherence processes. To efficiently excite atoms in a two-photon process to Rydberg state coherently, the Rabi frequencies of the two transitions have to be known and both Rabi frequencies have to match. We used this method to measure the Rabi frequency of the red laser by probing the  $5S_{1=2} \rightarrow 5P_{3=2}$  transition with the transition to the  $43S_{1=2}$  state (see fig. 7). By increasing the red laser intensity, the  $5S_{1=2} \rightarrow 5P_{3=2}$  transition splits up into two lines, where the splitting of the two lines is given by the Rabi frequency  $\nu_r = c_g \frac{I}{2I_s}$ . Here  $\nu$  is the linewidth of the transition,  $I$  the intensity of the laser and  $I_s$  the saturation intensity of the transition.  $c_g$  accounts for the polarization and state dependent coupling strength of the different possible transitions, which is based on the square of the Clebsch-Gordan coefficients. Since we excite in the MOT with a non-homogeneous magnetic field and an unpolarized atomic cloud, we have to use here a mean value for the  $5S_{1=2} \rightarrow 5P_{3=2}$  transition of  $c_g = 7=15$ . As shown in fig. 7, for a low intensity of  $2 I_s$  there is only one single line measured. By increasing the intensity, the line first broadens up and splits for higher intensities. From fig. 7 the measured Rabi frequency for an

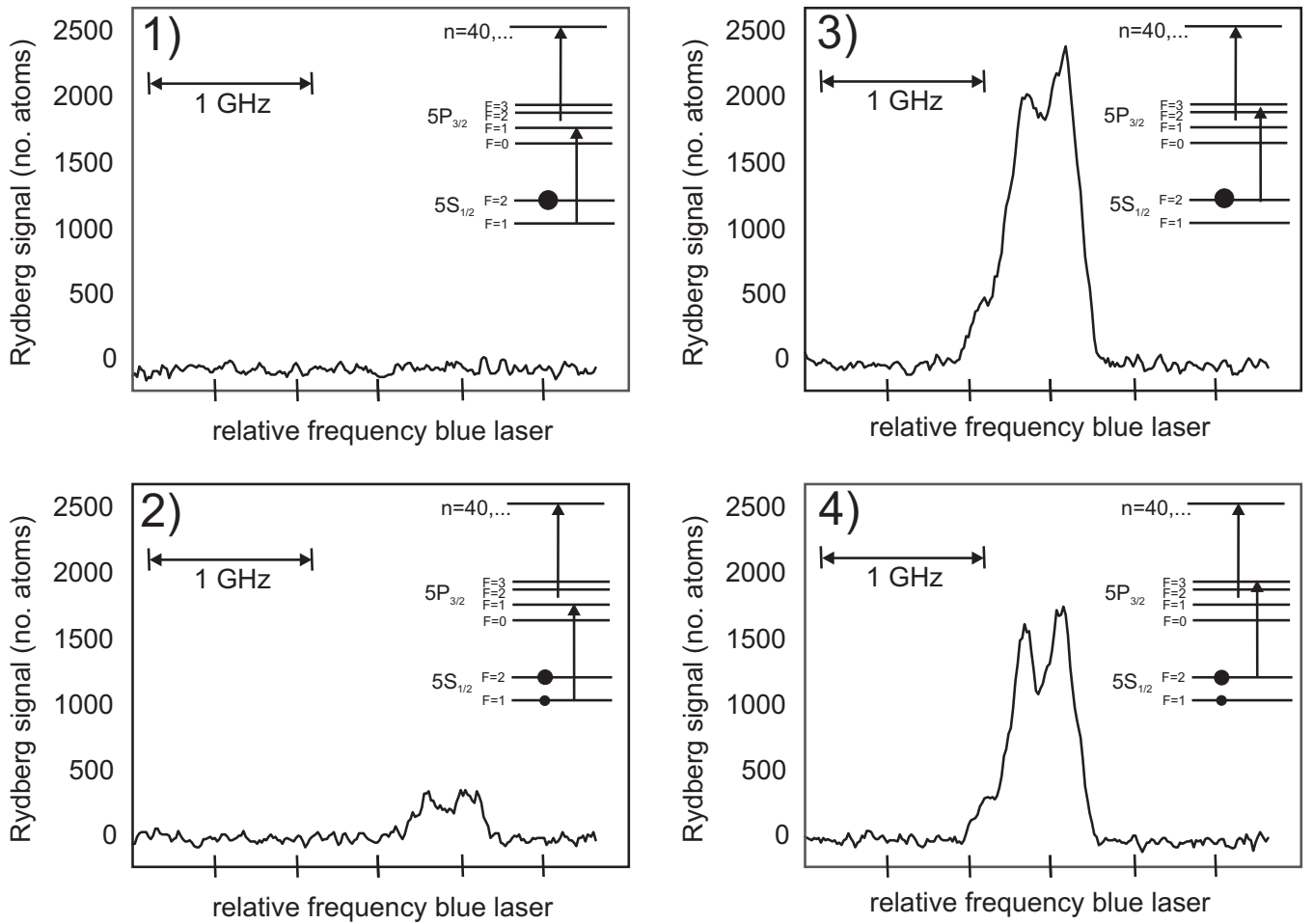


FIG. 6: State selective excitation of the Rydberg atoms from both the  $5S_{1/2}$  ( $F=1$ ) (1 and 2) and ( $F=2$ ) (3 and 4) states to the  $41D$  doublet. Without optical pumping of the atoms to the  $F=1$  state no Rydberg excitation is possible (1). With optical pumping before Rydberg excitation, atoms can be excited to a Rydberg state (2). Rydberg atom signal without optical pumping before Rydberg excitation (3) and with optical pumping of the atoms from the  $F=2$  to the  $F=1$  state (4).

intensity of  $151 I_s$  is 25 MHz. The calculated Rabi frequency of 24.6 MHz is in good agreement. The reason for the not identical height of both lines is that the red laser was slightly detuned with respect to the transition which results in a different strength of the lines.

## V I. CONCLUSION AND OUTLOOK

In this paper, we described a high resolution system for the excitation and investigation of  $^{87}\text{Rb}$  atoms in Rydberg states. All presented experiments were performed on an ensemble of ultracold atoms in a MOT. With this system, studies in the regime of a "frozen Rydberg gas" are possible. As first experiments, we tested the resolution and frequency stability of the system by the investigation of the Stark effect in the vicinity of the  $n=40$  Rydberg states. We could resolve the Stark effect of these states and even the field dependent splitting of the hyperfine states of both the  $43D_{3=2}$  and  $43D_{5=2}$  states. The smallest Rydberg lines we measured had a linewidth of 2.2 MHz which was limited by the broadening due to the MOT magnetic field.

To test the usability for quantum computing approaches, we excited both atoms spatial and state selectively to Rydberg states. We furthermore investigated the Autler-Townes splitting of the  $5S_{1/2} \rightarrow 5P_{3=2}$  transition which could be observed by probing this transition with an excitation to a Rydberg state.

In the next future, we will be able to start Rydberg excitation experiments on our  $^{87}\text{Rb}$  Bose-Einstein condensate. Furthermore an optical lattice is currently set up. So experiments on Rydberg excitation from atoms trapped inside an optical lattice will be possible, too.



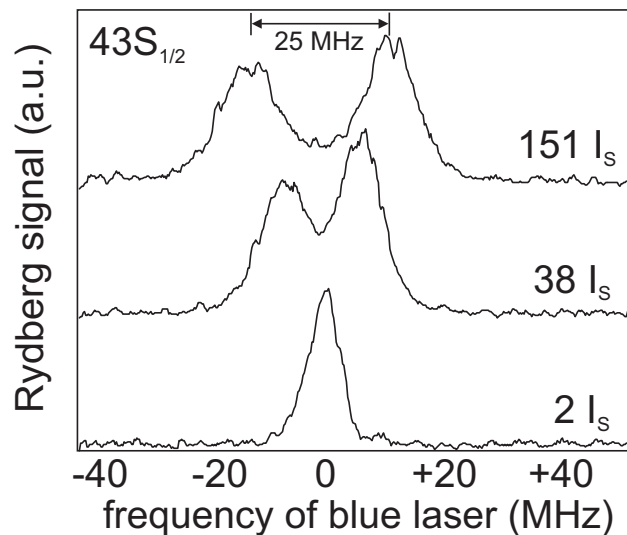


FIG. 7: A Autler-Townes splitting of the  $5S_{1=2}! \rightarrow 5P_{3=2}$  transition probed with a Rydberg transition to the  $43S_{1=2}$  state. For an intensity of  $151 I_s$  we get an Autler-Townes splitting of 25 MHz.

Acknowledgement We acknowledge financial support by the 'A8 Quantum Information Highway' programme of the Landesstiftung Baden-Württemberg

- 
- [1] T.F. Gallagher 1994, Rydberg Atoms (Cambridge: Cambridge University Press).
- [2] H.J.M.etcalf, and P.van der Straten, 1999, Laser Cooling and Trapping (New York, Springer Verlag).
- [3] W.R.Anderson, J.R.Veale, and T.F.Gallagher, Phys.Rev.Lett. 80, 249 (1998).
- [4] I.Mourachko, D.Comparat, F.de Tomasi, A.Fioretto, P.Nosbaum, V.M.Akulim, and P.Pillet, Phys.Rev.Lett. 80, 253 (1998).
- [5] K.Singer, M.Reetz-Lamour, T.Amthor, L.G.Marcassa, and M.Weidemuller, Phys.Rev.Lett. 93, 163001 (2004).
- [6] D.Tong, S.M.Farooqi, J.Stanojevic, S.Krishnan, Y.P.Zhang, R.Côte, E.E.Eyler, and P.L.Gould, Phys.Rev.Lett. 93, 063001 (2004).
- [7] T.J.Carroll, K.C.laringbould, A.Goodsell, M.J.Lin, and M.W.Noel, Phys.Rev.Lett. 93, 153001 (2004).
- [8] K.A.frousheh, P.Bohluli-Zanjani, D.Vagale, A.Mugford, M.Fedorov, and J.D.D.Martin, Phys.Rev.Lett. 93, 233001 (2004).
- [9] WenhuiLi, PaulJ.Tanner, and T.F.Gallagher, Phys.Rev.Lett. 94, 173001 (2005).
- [10] D.Jaksch, J.I.Cirac, P.Zoller, S.L.Rolston, R.Côte, and M.D.Lukin, Phys.Rev.Lett. 85, 2208 (2000).
- [11] M.D.Lukin, M.Fleischauer, R.Côte, L.M.Duan, D.Jaksch, J.I.Cirac, and P.Zoller, Phys.Rev.Lett. 87, 037901 (2001).
- [12] See, for example, R.Grimm, M.Weidemuller, and Y.B.Ovchinnikov, Adv.At.Mol.Opt.Phys. 42 95 (2000).
- [13] AxelGrabowski, and TilmanPfauf, Eur.Phys.JD 22, 347-354 (2003).
- [14] B.K.Teo, D.Feldbaum, T.Cubel, J.R.Guest, P.R.Berman, and G.Raithel, Phys.Rev.A 68, 053407 (2003).
- [15] J.Reichel, W.Hansel, and T.W.Hansch, Phys.Rev.Lett. B 83, 3398, (1999).
- [16] J.Reichel, W.Hansel, P.Hommelho, and T.W.Hansch, Appl.Phys.B 72, 81, (2001).
- [17] L.Riccib, M.Weidemuller, T.Esslinger, A.Hemmerich, C.Zimmermann, V.Vuletic, W.Konig, and T.W.Hansch, Optics Communications, 117,541 (1995).
- [18] W.Demtroder, 2002, Laser Spectroscopy, Berlin, Springer Verlag.
- [19] M.P.Robinson, B.LaburtheTolra, M.W.Noel, T.F.Gallagher, and P.Pillet, Phys.Rev.Lett. 85, 4466 (2000).
- [20] A.Walz-Flanigan, J.R.Guest, J.H.Chio, and G.Raithel, Phys.Rev.A 69, 063405 (2004).
- [21] C.Cohen-Tannoudji, J.Dupont-Roc, and G.Grynberg 1992, Atom-Photon Interactions (New York: Wiley-Interscience Publications).
- [22] S.H.Autler, and C.H.Townes, Phys.Rev. 100, 703 (1955).